Electronic Supplementary Material (ESI) for Nanoscale.

Electronic Supplementary Information

Hierarchical nickel–cobalt phosphide yolk-shell spheres as highly active and stable bifunctional electrocatalysts for overall water splitting

Zhuoxun Yin,[ac] Chunling Zhu,[b] Chunyan Li,[a] Shen Zhang,[a] Xitian Zhang[c] and Yujin Chen[a*]*

[a]Key Laboratory of In-Fiber Integrated Optics, Ministry of Education and College of Science, Harbin Engineering University, Harbin 150001, China. E-mail: chenyujin@hrbeu.edu.cn; Fax: +86-451-82519754; Tel: +86-451-82519754
[b]College of Materials Science and Chemical Engineering, Harbin Engineering University, Harbin 150001, China. E-mail: zhuchunling@hrbeu.edu.cn
[c]Key Laboratory for Photonic and Electronic Bandgap Materials, Ministry of Education,and School of Physics and Electronic Engineering, Harbin Normal University, Harbin 150025, China

*Corresponding authors.

E-mail addresses: chenyujin@hrbeu.edu.cn and zhuchunling@hrbeu.edu.cn

Tel.: +086-0451-82519754, Fax: +086-0451-82519754

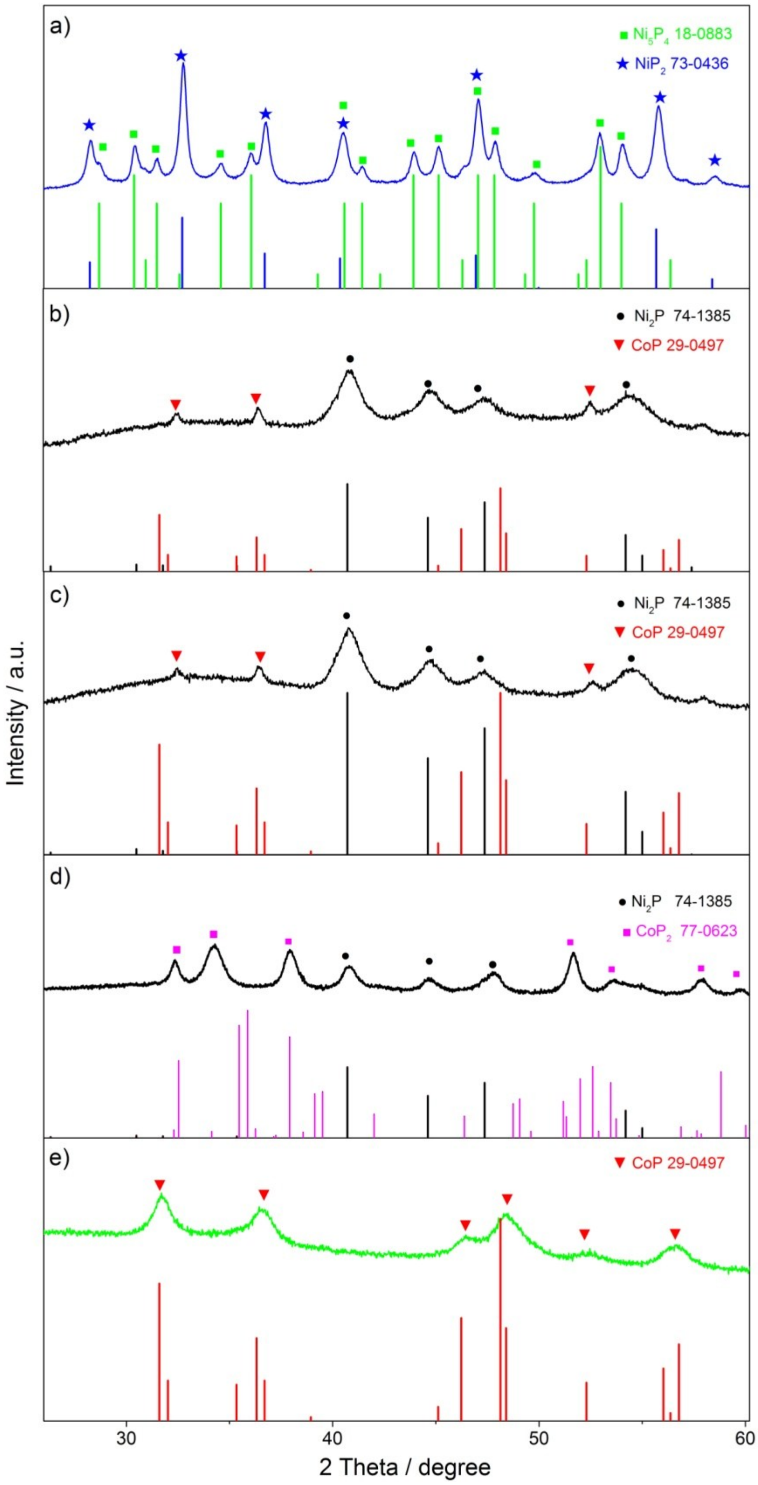

Figure S1 XRD pattern of (a) Ni–P (b) $Ni_{0.78}Co_{0.22}$–P (c) $Ni_{0.69}Co_{0.31}$–P (d) $Ni_{0.54}Co_{0.46}$–P (e) Co–P.

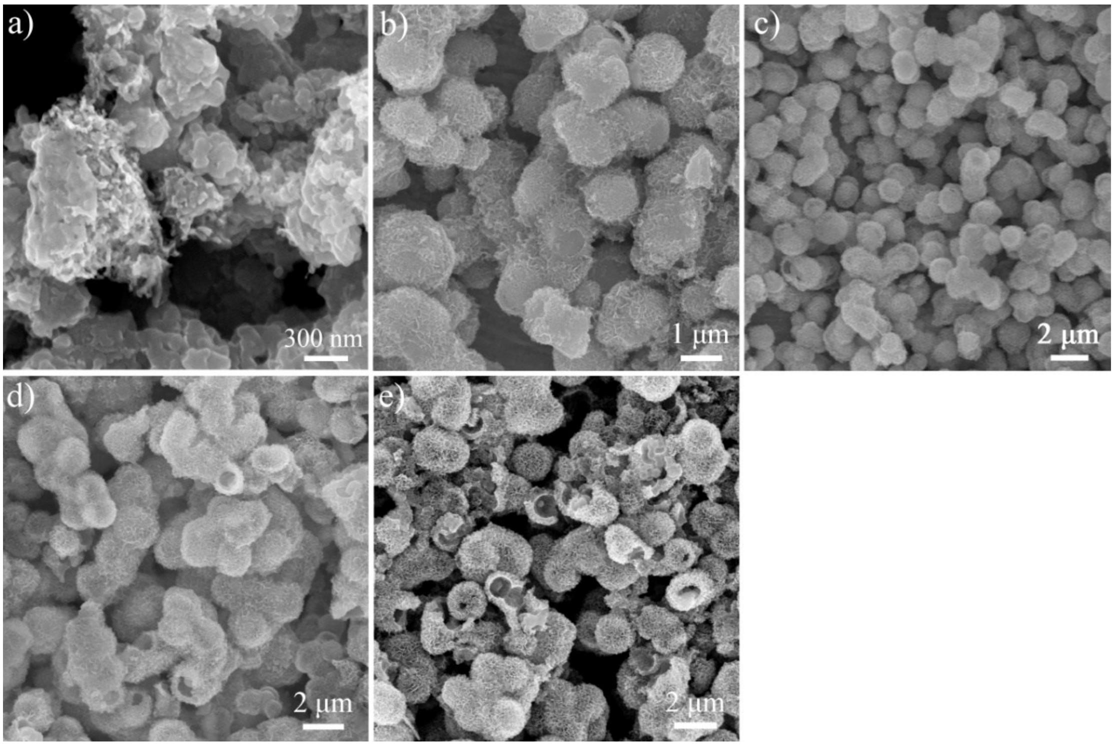

Figure S2 SEM images of (a) Ni–P (b) $Ni_{0.78}Co_{0.22}$–P (c) $Ni_{0.69}Co_{0.31}$–P (d) $Ni_{0.54}Co_{0.46}$–P (e) Co–P.

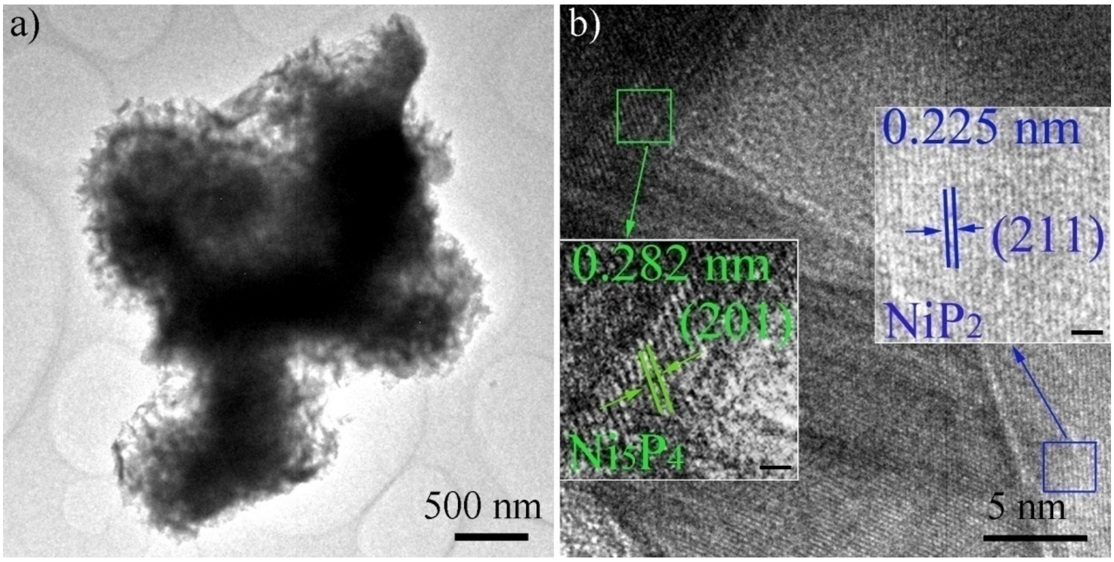

Figure S3 TEM images of Ni–P catalysts. a) Low-magnification TEM image, and b) HRTEM image. Inset in b) shows the interplanar distances at marked regions.

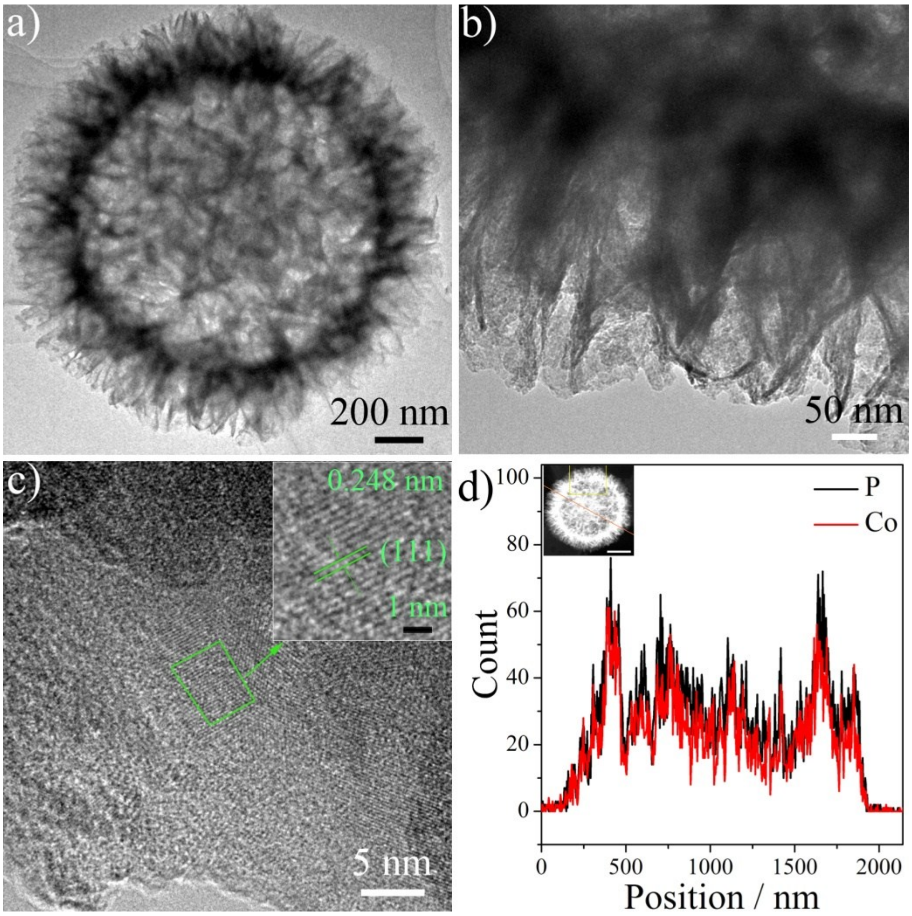

Figure S4 TEM images of Co–P catalysts. a) Low-magnification TEM image, b) high-magnification TEM image of the outmost layer, c) HRTEM image, and inset shows lattice fringes of marked region, d) linear scanning EDX mapping and the inset shows the corresponding ADF STEM image.

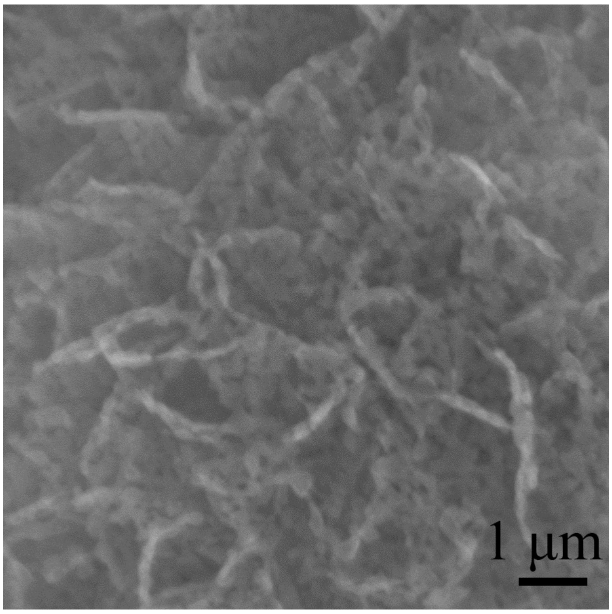

Figure S5 High-magnification SEM image of the outmost layers of $Ni_{0.69}Co_{0.31}$–P catalysts.

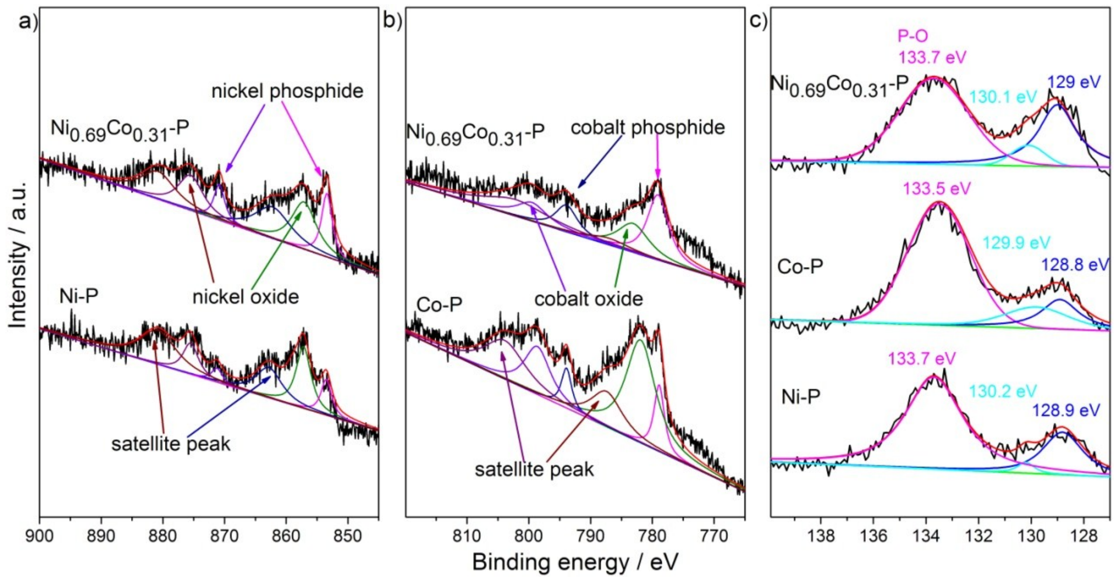

Figure S6 Comparison of XPS spectrum of Ni–P, $Ni_{0.69}Co_{0.31}$–P and Co–P catalysts. a) Ni 2p, b) Co 2p and c) P 2p.

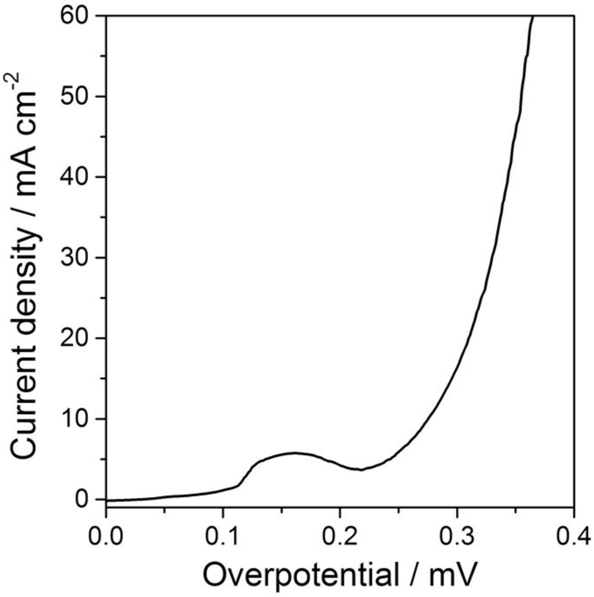

Figure S7 Polarization curves of $Ni_{0.69}Co_{0.31}$–P catalysts at a scan rate of 0.2 mV s^{-1} in 0.1 M KOH

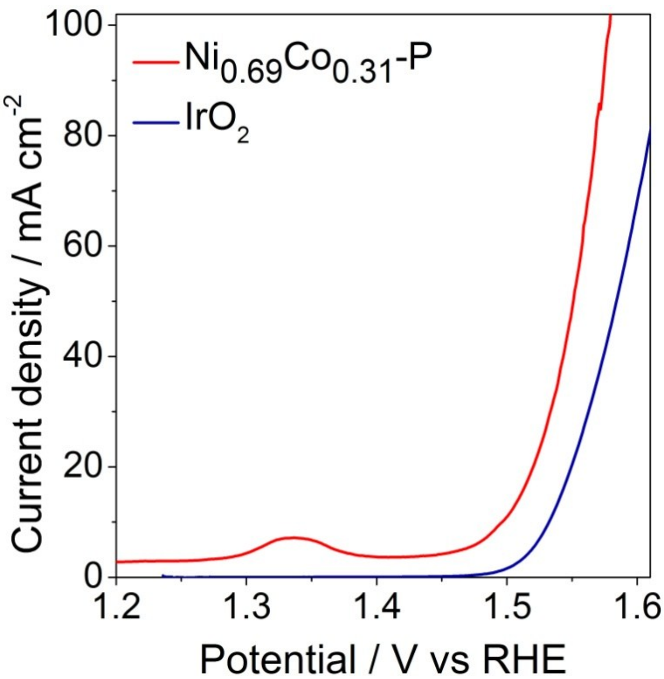

Figure S8 Polarization curves of $Ni_{0.69}Co_{0.31}$–P and IrO_2 catalysts at a scan rate of 0.2 mV s^{-1} in 1 M KOH

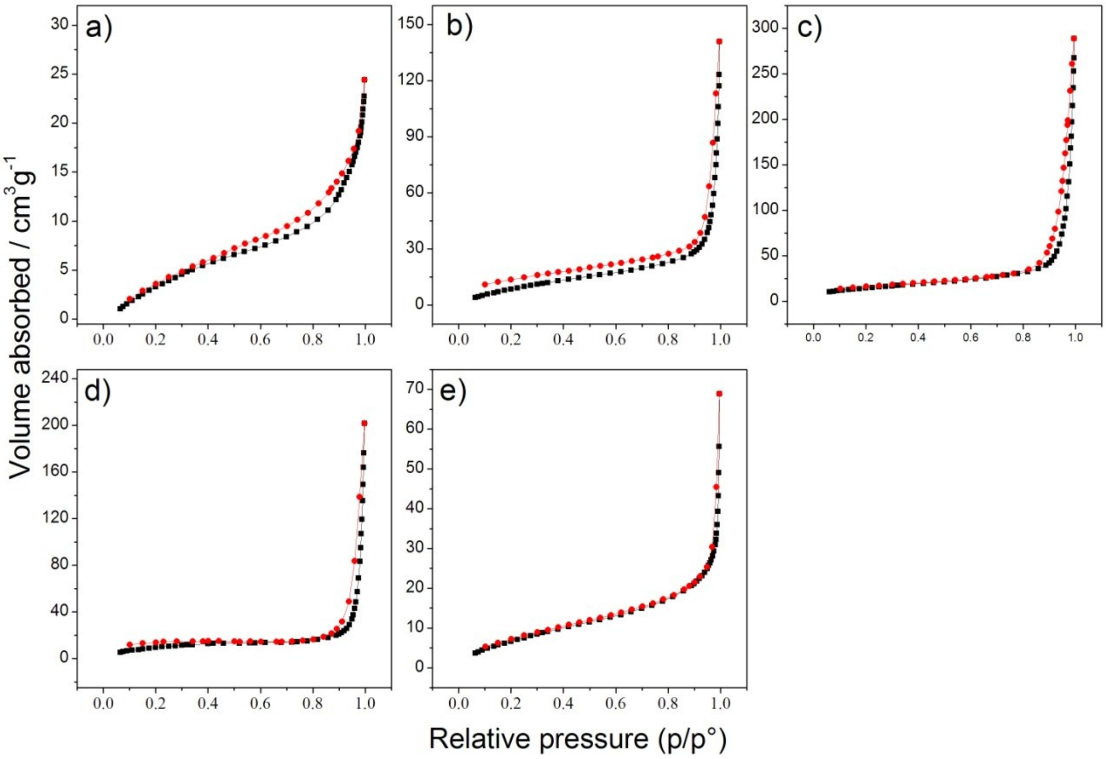

Figure S9 Nitrogen adsorption and desorption isotherms of (a) Ni–P (b) $Ni_{0.78}Co_{0.22}$–P (c) $Ni_{0.69}Co_{0.31}$–P (d) $Ni_{0.54}Co_{0.46}$–P (e) Co–P.

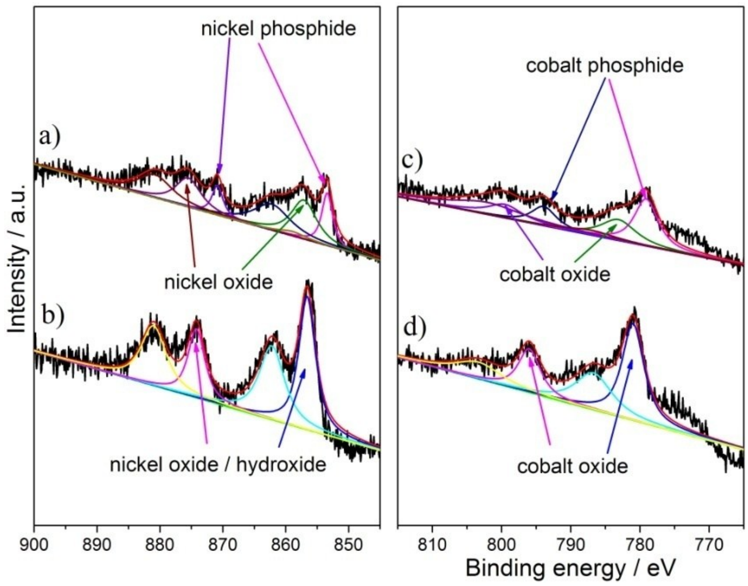

Figure S10 Comparison of XPS spectrum of $Ni_{0.69}Co_{0.31}$–P before and after OER process. a, b) Ni 2p, c, d) Co 2p.

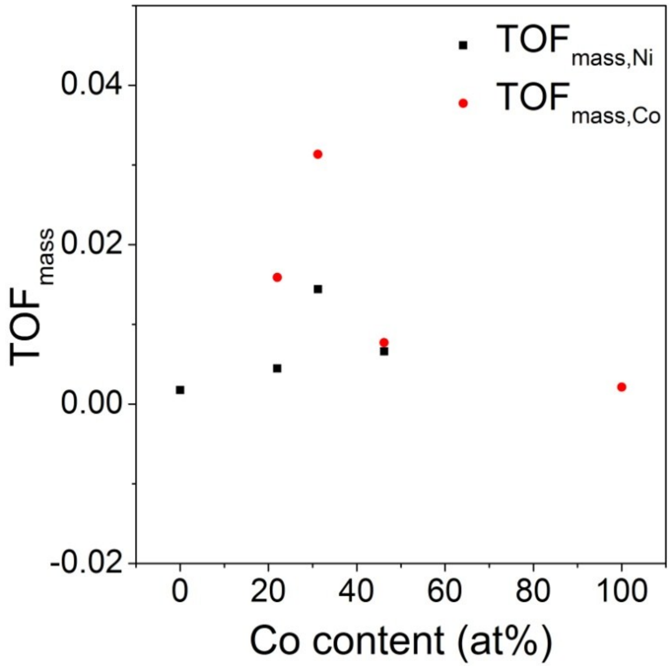

Figure S11 TOF data for $Ni_{1-x}Co_x$–P catalysts is calculated based on the number of metal atoms.

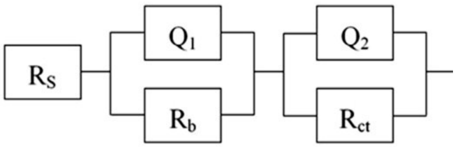

Figure S12 The equivalent circuit for Nyquist plots of the $Ni_{1-x}Co_x$–P electrodes.

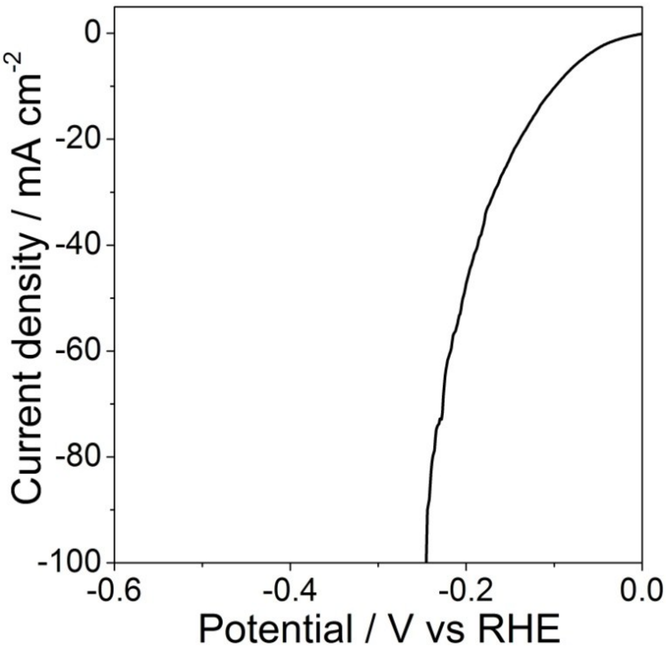

Figure S13 Polarization curves of $Ni_{0.69}Co_{0.31}$–P catalysts for HER at a scan rate of 5 mV s^{-1} in 0.1 M KOH

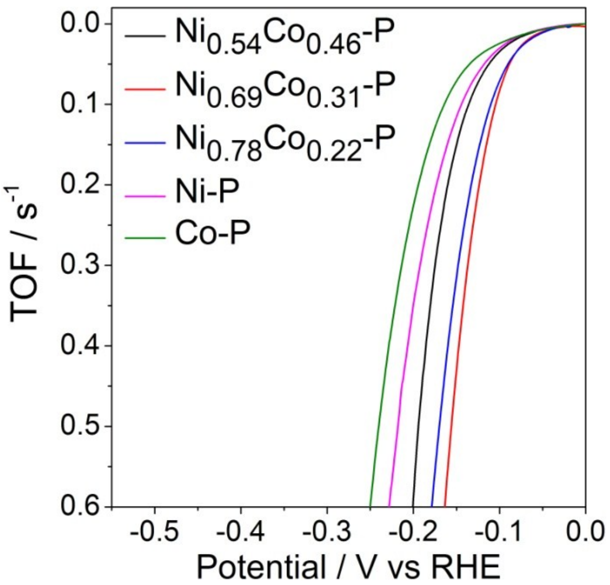

Figure S14 The TOFs of the $Ni_{1-x}Co_x$–P catalysts at different potentials in 1.0 M KOH

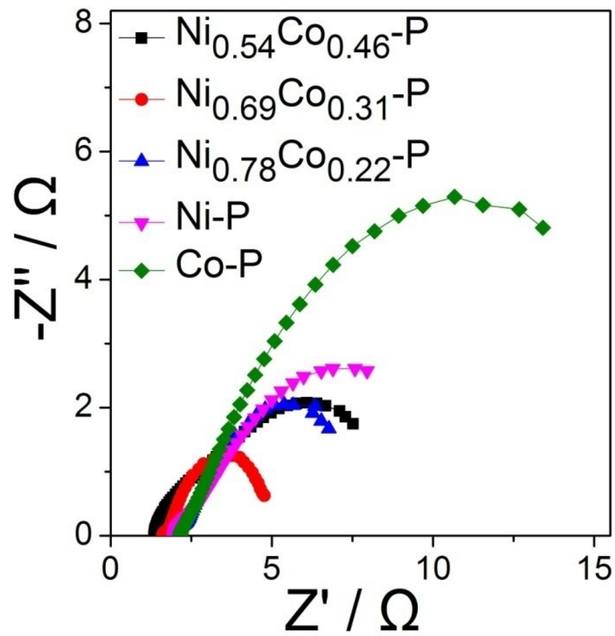

Figure S15 Nyquist plots of the $Ni_{1-x}Co_x$–P catalysts at η_{HER} of 100 mV

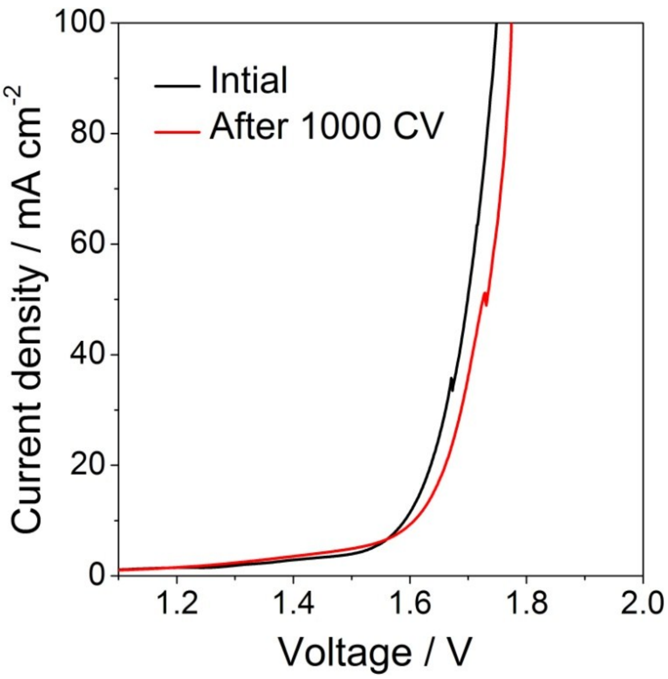

Figure S16 Stability test for the $Ni_{0.69}Co_{0.31}$–P|$Ni_{0.69}Co_{0.31}$–P catalysts by CV scanning for 1000 cycles in 1.0 M KOH solution at a scan rate of 50 mV s^{-1}

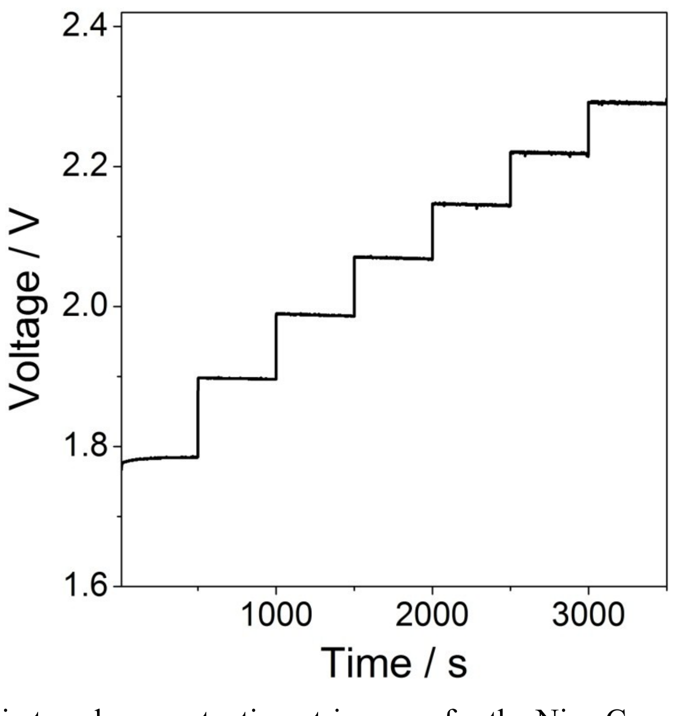

Figure S17 Multi-step chronopotentiometric curve for the $Ni_{0.69}Co_{0.31}$–P|$Ni_{0.69}Co_{0.31}$–P catalysts in 1.0 M KOH solution

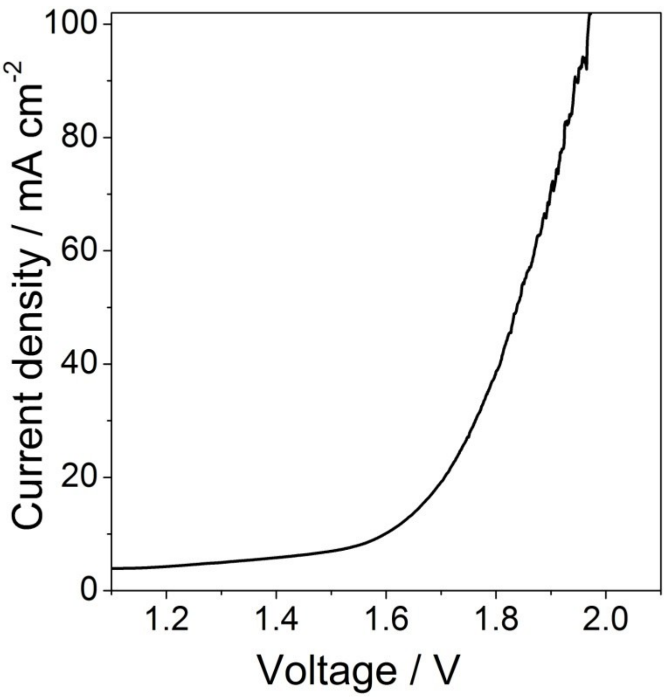

Figure S18 Polarization curves of $Ni_{0.69}Co_{0.31}$–P∣$Ni_{0.69}Co_{0.31}$–P at a scan rate of 1 mV s^{-1} in 0.1 M KOH

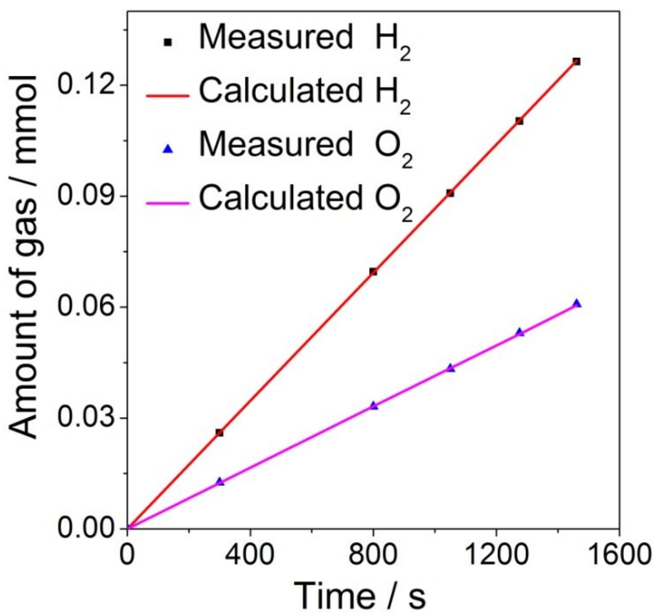

Figure S19 The amount of gas theoretically calculated and experimentally measured versus time for overall water splitting of $Ni_{0.69}Co_{0.31}$–P∣$Ni_{0.69}Co_{0.31}$–P

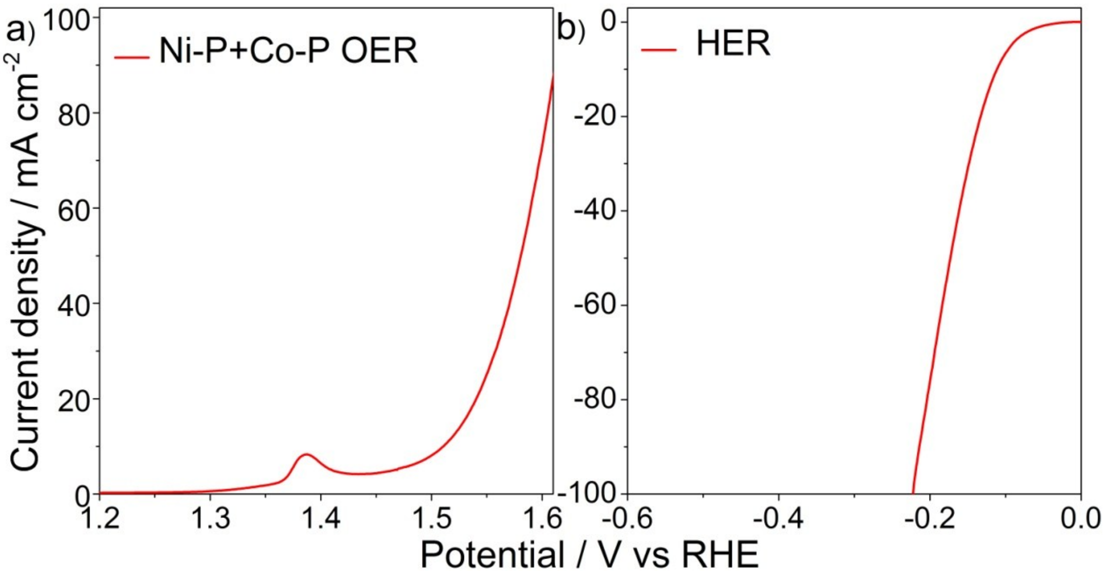

Figure S20 a) Polarization curves of Ni–P+Co–P catalysts for OER at a scan rate of 0.2 mV s^{-1} in 1.0 M KOH, and b) Polarization curves of Ni–P+Co–P catalysts for HER at a scan rate of 5 mV s^{-1} in 1.0 M KOH

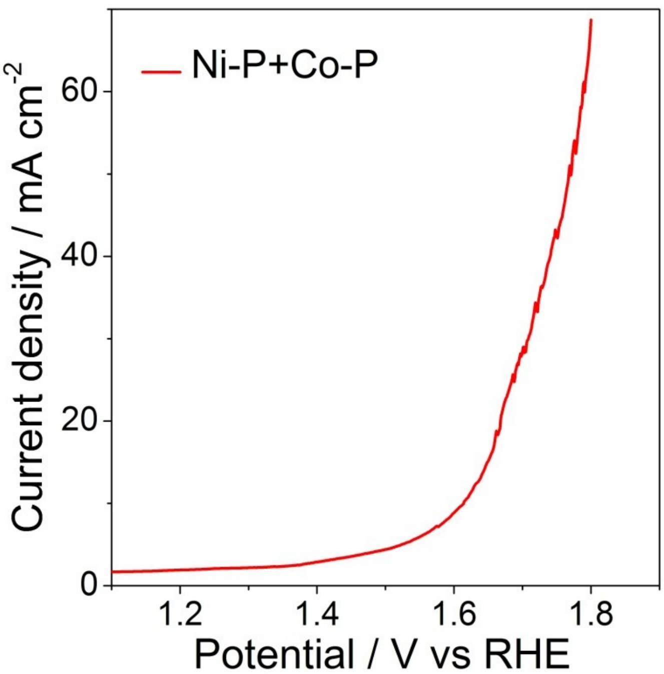

Figure S21 Polarization curves for the Ni–P+Co–P│Ni–P+Co–P at a scan rate of 1 mV s^{-1} in 1.0 M KOH

Table S1 Determination of x by EDS and ICP-OES (x = n_{Co}/n_{Ni+Co}, n molar number)

Catalysts	$Ni_{0.78}Co_{0.22}$-P	$Ni_{0.69}Co_{0.31}$-P	$Ni_{0.54}Co_{0.46}$-P
x determined by EDS	0.23	0.33	0.48
x determined by ICP-OES	0.21	0.29	0.44
Average value	0.22	0.31	0.46

Table S2 Comparison of OER activity data among different catalysts.

Catalysts	Overpotential at 10 mA cm^{-2} (mV vs RHE)	Current density at 350 mV (mA cm^{-2})	Electrolyte concentration (pH)	Ref.
$Ni_{0.69}Co_{0.31}$-P	**266**	**104**	14	This work
$Ni_{0.69}Co_{0.31}$-P	**276**	**45.5**	13	This work
FeNC sheets/NiO	390	4	13	7
Co_3O_4C-NA	290	＜29	13	8
Au@Co_3O_4	≈390	2.84	13	12
NiO_x	—	20 (370 mV)	14	15
MnO/Au-GC	≈570	0.23 (400mV)	13	17
CoO_x-(a)	390	0.9 ± 0.3	14	18
CoO_x-(b) ("CoPi")	420	0.4 ± 0.1	14	18
$CoFeO_x$	370	7 ± 3	14	18
NiO	420	1.1 ± 0.4	14	18
$NiCeO_x$	430	1.6 ± 0.7	14	18
$NiCoO_x$	380	6 ± 3	14	18
$NiCuO_x$	410	1.4 ± 0.6	14	18
$NiFeO_x$	350	15 ± 6	14	18
$NiLaO_x$	410	2.5 ± 0.9	14	18

FeO_x/CFC	545	—	14	20
$Ni(OH)_2$ films@Au	280	—	14	23
CoCo-B	390	2.019	14	25
CoCo-NS	353	8.628	14	25
NiCo-B	385	3.036	14	25
NiCo-NS	334	22.78	14	25
NiFe-B	347	10.75	14	25
MWCNTs/$Ni(OH)_2$	474	—	13	27
NiOOH	＞300	15	14	30
$Fe_6Ni_{10}O_x$	286	—	14	31
Ni −Fe films	280	—	13	32
n-NiFe LDH /NGF	337	＜7.5	13	35
Ni-Co binary oxide NPL	325	—	14	45
$NiCo_2O_4$ hollow microcuboids	290	＜100	14	46
PNG-NiCo	＞417	＜10	14	47
Ni@[$Ni^{(2+/3+)}$ Co_2 $(OH)_{6–7}$]$_x$ nanotube arrays	460	—	14	48
NiCo LDH nanosheets	367	＜7	14	49
$NiCo_{2.7}$ $(OH)_x$	350	10	14	50
Ni-$CoMoO_4$	300	—	14	52

CoMn LDH	324	42.5	14	53
$Co_3O_4/NiCo_2O_4$ DSNCs	340	＜22	14	54
$NiOOH/Ni_5P_4$	290	＜60	14	58
Ni_2P nanowires	290	—	14	59
CoP/C	360	＜20	13	60
CoP −CNT	330	—	13	61
CoP hollow polyhedron	400	＜5	14	62
CoP based nanoneedle arrays	281	—	14	63
CoP/rGO	340	＜20	14	64
Co-P film	345	＜20	14	65
nickel–phosphorous films	344	＜20	14	67
Ni_2P NWs	400	＜5	14	70
Ni-P	300	—	14	71
NG-$CoSe_2$	366	＜8	13	76

Table S3 Comparison of HER activity data among different catalysts.

Catalyst	Tafel slope (mV dec^{-1})	Overpotential at 10 mA cm^{-2} (mV vs RHE)	Overpotential at 100 mA cm^{-2} (mV vs RHE)	Electrolyte concentration (pH)	Ref.
$Ni_{0.69}Co_{0.31}$-P	47	96	167	14	This work
Co@CoO/NG	122	82	221	14	19
$NiCo_2O_4$ Hollow Microcuboids	49.7	110	245	14	46
NiSe/NF	43	96	＞200	14	55
CoOx@CN	—	—	＞200	14	56
PCPTF	—	＞350	＞500	14	57
Ni_5P_4	—	150		14	58
CoP/C	—	＞200	＞250	14	60
CoP hollow polyhedron	59	159	＞300	0	62
CoP-based nanoneedle arrays	69	114	＞200	14	63
CoP/rGO-400	38	150	＞250	14	64
Co-P film	42	94	—	14	65
CoP NCs	46	—	180	0	72
MoP_2 NS/CC	63.6	115	—	0	74

Table S4 Comparison of the electrochemical performance of $Ni_{0.69}Co_{0.31}$–P|$Ni_{0.69}Co_{0.31}$–P as bifunctional catalysts for overall water splitting in 1.0 M KOH with recently published results.

Catalyst	Voltage at 10 mA cm^{-2}(V)	Voltage at 100 mA cm^{-2}(V)	Electrolyte concentration (pH)	Ref.
$Ni_{0.69}Co_{0.31}$-P	1.59	1.749	14	This work
Co@CoO/NG	1.6	1.7	14	19
$NiCo_2O_4$ Hollow Microcuboids	1.65	—	14	46
NiSe/NF	1.63	>2	14	55
CoOx@CN	1.55	—	14	56
Ni_5P_4	1.7	>2.1	14	58
Ni_2P	1.63	>1.75	14	59
CoP-based nanoneedle	1.61	>1.75	14	63
CoP/rGO-400	1.7	>1.8	14	64
Co-P	>1.6	1.744	14	65
Ni–P	1.67	>1.8	14	67
Ni–P foam	1.64	2.05	14	68

Table S5 Comparison of the electrochemical performance of $Ni_{0.69}Co_{0.31}$–P and Ni–P+C–P catalysts

Catalyst	OER	HER	overall water splitting
	Overpotential at 10 mA cm^{-2} (mV vs RHE)	Overpotential at 10 mA cm^{-2} (mV vs RHE)	Voltage at 10 mA cm^{-2}
$Ni_{0.69}Co_{0.31}$-P	266	96	1.59
Ni–P+C–P	291	112	1.62